Generic behavior of master-stability functions in coupled nonlinear dynamical systems

Liang Huang,[1] Qingfei Chen,[1] Ying-Cheng Lai,[1,2] and Louis M. Pecora[3]
[1]*School of Electrical, Computer and Energy Engineering, Arizona State University, Tempe, Arizona 85287, USA*
[2]*Department of Physics, Arizona State University, Tempe, Arizona 85287, USA*
[3]*Code 6362, Naval Research Laboratory, Washington, DC 20375, USA*
(Received 9 June 2009; published 15 September 2009)

Master-stability functions (MSFs) are fundamental to the study of synchronization in complex dynamical systems. For example, for a coupled oscillator network, a necessary condition for synchronization to occur is that the MSF at the corresponding normalized coupling parameters be negative. To understand the typical behaviors of the MSF for various chaotic oscillators is key to predicting the collective dynamics of a network of these oscillators. We address this issue by examining, systematically, MSFs for known chaotic oscillators. Our computations and analysis indicate that it is generic for MSFs being negative in a finite interval of a normalized coupling parameter. A general scheme is proposed to classify the typical behaviors of MSFs into four categories. These results are verified by direct simulations of synchronous dynamics on networks of actual coupled oscillators.

DOI: 10.1103/PhysRevE.80.036204 PACS number(s): 05.45.−a, 84.30.Ng

I. INTRODUCTION

Synchronization in complex dynamical systems has been a topic of continuous interest [1–8]. A basic tool in the analyses of various synchronization problems is the master-stability function (MSF) [6]. Given a complex dynamical system consisting of a number of identical coupled oscillators, a synchronous solution can arise whereas the dynamical variables of all oscillators approach each other asymptotically. Due to the entrainment of dynamical variables from different components, which in the absence of coupling would behave independently, the dimension of the subspace in which the synchronous solution lies is necessarily much smaller than the dimension of the full phase space. Mathematically, the synchronous subspace is termed the synchronization manifold. Whether the manifold is stable with respect to perturbations in the complementary subspace or the transverse subspace determines whether synchronization can be observed in a physical environment. The MSF measures the exponential rate at which an infinitesimal perturbation in the transverse subspace grows. In the terminology of dynamical systems, MSF is the largest transverse Lyapunov exponent of the synchronization manifold [6]. A necessary condition for synchronization to occur is that the MSF be negative and the corresponding normalized coupling parameters (determined by the coupled oscillator system) fall in the negative region of the MSF.

In 2002, the MSF formalism was applied [9] to analyzing the synchronizability of small-world networks [10]. This marks the beginning of an explosively growing area of research in nonlinear science and engineering: synchronization in complex networks [11–18]. The MSF formalism is appealing because it allows the properties of the local oscillators to be separated from the coupling matrix characterizing the topology of the underlying network. In particular, let K be a normalized coupling parameter so that the MSF can be calculated as a function of K, based only on knowledge about the dynamics of the individual oscillators and the coupling function. That is, the MSF can be obtained independent of the topology of the underlying network that supports a large number of such oscillators. A tacit assumption in the network-synchronization literature is that the MSF is negative in some interval, (K_a, K_b), where $K_a < K_b$. The network is synchronizable if all nonzero quantities $K_i \equiv \varepsilon\mu_i (i = 2, \ldots, N)$ fall in the interval, where ε is a coupling parameter characterizing the average interaction among oscillators, μ_is are the eigenvalues of the coupling matrix, N is the number of oscillators in the network, and $\mu_1 = 0$ is assumed. Given the interval (K_a, K_b), a network of a specific topology is more likely to be synchronized if the spread of the nontrivial eigenvalue spectrum is smaller.

A question is whether the property of the existence of intervals of negative MSF values holds for typical nonlinear oscillators. In general, this question is difficult to address as there are an infinite number of possibilities for oscillatory dynamics. To be realistic, we ask the following question: among typical low-dimensional dynamical oscillators known to the nonlinear-dynamics community, does the aforementioned property of the MSF hold? In this paper, we shall then examine, systematically, an array of known dynamical oscillators ranging from the chaotic Rössler oscillator [19], the Lorenz oscillator [20], and its generalization [21] to chaotic Chua's circuits [22] and Hindmarsh-Rose (HR) neuron [23]. We have also examined two driven oscillators, the Duffing oscillator [24] and the van der Pol oscillator [25]. Our extensive computations and analyses lend strong credence to the proposition that it is a generic property of the MSF to be negative in a *finite* parameter interval. The implication is that, for any of these oscillators, there always exists a coupling scheme for which network synchronization of a large number of such oscillators can be realized. We also provide a general scheme to classify the behaviors of MSFs into four categories.

In Sec. II, we briefly review the basics of MSF-based analysis. In Sec. III, we present systematic numerical results for MSFs for typical nonlinear dynamical oscillators with different coupling schemes. A heuristic analysis is provided in Sec. IV to shed light on the generic behavior of MSFs in the large coupling limit. In Sec. V, we provide numerical

simulations of actual coupled oscillator networks to validate the MSF-based analysis. A brief conclusion is offered in Sec. VI.

II. SYNCHRONIZATION ANALYSIS BASED ON MSFS

We consider a complex dynamical system consisting of coupled continuous-time nonlinear oscillators. Because of the intrinsic nonlinearity underlying each individual oscillator, chaotic behaviors are common. Each oscillator when isolated is described by

$$\frac{d\mathbf{x}}{dt} = \mathbf{F}(\mathbf{x}), \tag{1}$$

where $\mathbf{x}$ is a d-dimensional vector and $\mathbf{F}(\mathbf{x})$ is the velocity field. To be general, we address chaotic synchronization by choosing the parameters of each oscillator such that it exhibits a chaotic attractor. The typical setting in the literature for the dynamics of a network of N coupled oscillators is

$$\frac{d\mathbf{x}_i}{dt} = \mathbf{F}(\mathbf{x}_i) - \varepsilon \sum_{j=1}^{N} G_{ij}\mathbf{H}(\mathbf{x}_j), \tag{2}$$

where $\mathbf{H}(\mathbf{x})$ is a coupling function, ε is a global coupling parameter, and $\mathbf{G}$ is a coupling matrix determined by the connection topology. The matrix $\mathbf{G}$ satisfies the condition $\Sigma_{j=1}^{N} G_{ij}=0$ for any i, where N is the network size. As a consequence, the synchronous state $\mathbf{x}_1=\mathbf{x}_2=\cdots=\mathbf{x}_N=\mathbf{s}$, where $d\mathbf{s}/dt=\mathbf{F}(\mathbf{s})$ is an exact solution of Eq. (2). Furthermore, we assume that the coupling matrix $\mathbf{G}$ can be diagonalized with a set of real eigenvalues $\{\mu_i, i=1,\ldots,N\}$ and their respective normalized eigenvectors $\mathbf{e}_1,\mathbf{e}_2,\ldots,\mathbf{e}_N$ [26]. The network is connected so there is only one zero eigenvalue such that the eigenvalues can be sorted as $0=\mu_1<\mu_2\leq\cdots\leq\mu_N$ [27].

For the system described by Eq. (2), the variational equations governing the time evolution of the set of infinitesimal vectors about the synchronous solution $\delta\mathbf{x}_i(t)\equiv\mathbf{x}_i(t)-\mathbf{s}(t)$ are

$$\frac{d\delta\mathbf{x}_i}{dt} = \mathbf{DF}(\mathbf{s})\cdot\delta\mathbf{x}_i - \varepsilon\sum_{j=1}^{N} G_{ij}\mathbf{DH}(\mathbf{s})\cdot\delta\mathbf{x}_j, \tag{3}$$

where $\mathbf{DF}(\mathbf{s})$ and $\mathbf{DH}(\mathbf{s})$ are the $d\times d$ Jacobian matrices of the corresponding vector functions evaluated at $\mathbf{s}(t)$. The transform $\delta\mathbf{y}=\mathbf{Q}^{-1}\cdot\delta\mathbf{x}$, where $\mathbf{Q}$ is a matrix whose columns are the set of eigenvectors of $\mathbf{G}$, leads to the block-diagonally decoupled form of Eq. (3):

$$\frac{d\delta\mathbf{y}_i}{dt} = [\mathbf{DF}(\mathbf{s}) - \varepsilon\mu_i\mathbf{DH}(\mathbf{s})]\cdot\delta\mathbf{y}_i.$$

Letting $K_i=\varepsilon\mu_i(i=2,\ldots,N)$ be a specific set of values of a normalized coupling parameter K, each block of the above decoupled equation is structurally the same with only the factor of K_i being different. This leads to the generic form for all the decoupled blocks:

$$\frac{d\delta\mathbf{y}}{dt} = [\mathbf{DF}(\mathbf{s}) - K\mathbf{DH}(\mathbf{s})]\cdot\delta\mathbf{y}. \tag{4}$$

The largest Lyapunov exponent determined from Eq. (4) is the MSF $\Psi(K)$ [6]. If $\Psi(K)$ is negative, a small disturbance from the synchronization state will diminish exponentially so that the synchronous solution is stable, at least when the oscillators are initialized in its vicinity. The synchronous solution is unstable and cannot be realized physically if $\Psi(K)$ is positive because small perturbations from the synchronous state will lead to trajectories that diverge from the state. For the coupled oscillator network [Eq. (2)], a necessary condition for synchronization is then that all normalized coupling parameters $K_i(i=2,\ldots,N)$ fall in an interval on the K axis where $\Psi(K)$ is negative. A network is more synchronizable if the spread in the set of K_i values (or equivalently, the spread in the eigenvalue spectrum μ_i) is smaller.

For nonlinear oscillators, the Jacobian matrix $\mathbf{DF}$ typically depends on the trajectory $\mathbf{s}(t)$. For linear coupling function $\mathbf{H}(\mathbf{x})$, the corresponding Jacobian matrix $\mathbf{DH}$ is a constant matrix. To be concrete, we consider the physically meaningful coupling scheme where oscillators interact with each other through only one component. To be as general as possible, we shall study all possible one-component couplings, e.g., the situation where the ith component of one oscillator coupled to the jth component of another oscillator: $[\mathbf{H}(\mathbf{x})]_k=\delta_{jk}x_i$, where δ_{jk} is the Kronecker's delta such that $\delta_{jk}=1$ if $j=k$ and zero otherwise, and i and j are running indices from 1 to d. The Jacobian matrix $\mathbf{DH}$ thus has one nonzero element only: $(\mathbf{DH})_{ji}=1$, while all other elements are zero.

III. MSFs FOR TYPICAL NONLINEAR SYSTEMS

A. Numerical procedure

The Lyapunov exponents determined by the variational Eq. (4) are calculated as follows. We define $\widetilde{\mathbf{DF}}(\mathbf{s})=\mathbf{DF}(\mathbf{s})-K\mathbf{DH}(\mathbf{s})$ and then consider the matrix equation

$$\frac{d\mathbf{O}(t)}{dt} = \widetilde{\mathbf{DF}}(\mathbf{s})\cdot\mathbf{O}(t) \tag{5}$$

with initial condition $\mathbf{O}(0)=\mathbf{I}$, where $\mathbf{I}$ is the identical matrix of order d [28]. This matrix equation is solved together with Eq. (1) that yields the trajectory $\mathbf{s}(t)$. Both equations are integrated using the same routine, e.g., the fourth-order Runge-Kutta (RK4) method (the calculated Lyapunov exponents will have systematic deviations if, for instance, the system state is integrated using RK4 while the matrix equation is integrated using a different routine). Let $\nu_i(t)(i=1,\ldots,d)$ be the eigenvalues of $\mathbf{O}(t)$. The Lyapunov exponents are given by

$$\lambda_i = \lim_{t\to\infty}\frac{1}{t}\ln\,\nu_i(t). \tag{6}$$

Numerically integrating Eq. (5) for relatively long time is not practical as the solution will quickly diverge when the system has a positive Lyapunov exponent or it will diminish to the computer round-off if all Lyapunov exponents are negative. A necessary remedy is to "normalize" and reset $\mathbf{O}(t)$ periodically so that the Lyapunov exponents can be obtained from the normalization parameters. We use the QR decomposition method to "normalize" $\mathbf{O}(t)$ [29]. In our computa-

tion, 10^4 cycles of $\mathbf{s}(t)$ are first integrated to allow the system to settle into an attractor. Then, 3×10^4 cycles are used to calculate Lyapunov exponents. Time step is chosen to be $dt=0.001$.

For special cases where $\widetilde{\mathbf{DF}}(\mathbf{s})$ can be approximated by a constant matrix $\mathbf{C}$, which can be diagonalized, $\mathbf{C}=\mathbf{P}^{-1}\mathbf{\Omega}\mathbf{P}$, where $\mathbf{\Omega}=\mathrm{diag}[\omega_1,\ldots,\omega_d]$ is the eigenvalue matrix. The constant matrix $\mathbf{P}$ needs not to be orthogonal. Equation (5) can be rewritten as

$$\frac{d\mathbf{O}(t)}{dt}=\mathbf{P}^{-1}\mathbf{\Omega}\mathbf{P}\cdot\mathbf{O}(t)$$

or equivalently

$$\frac{d\mathbf{PO}(t)}{dt}=\mathbf{\Omega}\cdot\mathbf{PO}(t).$$

The solution is given by $\mathbf{PO}(t)=e^{\mathbf{\Omega}t}\mathbf{PO}(0)=e^{\mathbf{\Omega}t}\mathbf{P}$ or $\mathbf{O}(t)=\mathbf{P}^{-1}e^{\mathbf{\Omega}t}\mathbf{P}$. Thus $\nu_i(t)=e^{\omega_i t}$. From Eq. (6), we have

$$\lambda_i=\lim_{t\to\infty}\frac{1}{t}\ln e^{\omega_i t}=\mathrm{Re}\ \omega_i.$$

B. Numerical results from typical nonlinear oscillators

We calculate the MSFs for typical low-dimensional nonlinear oscillators under all possible one-component coupling configurations. In particular, for a three-dimensional system described by dynamical variables (x_1,x_2,x_3), there are nine linear coupling configurations: $1\to1$, $1\to2$, $1\to3$, $2\to1$, $2\to2$, $2\to3$, $3\to1$, $3\to2$, and $3\to3$, and we calculate the MSFs for all these configurations. [Here the notation $i\to j(i,j=1,2,3)$ stands for the coupling scheme from the ith component of one oscillator to the jth component of another oscillator.] We shall present results with the following seven nonlinear oscillators: Rössler oscillator, Lorenz oscillator, Chua's circuit, Chen's oscillator, HR neuron, the forced Duffing's oscillator, and the forced van der Pol oscillator. In all cases, the parameters are adopted from literature (see reference for each case) where the resulting attractor is chaotic so that it possesses one positive Lyapunov exponent, which is $\Psi(0)$.

1. Rössler system

Here,

$$\begin{cases}\dot{x}=-y-z,\\ \dot{y}=x+\alpha y,\\ \dot{z}=\beta+(x-\gamma)z,\end{cases}\tag{7}$$

where the parameters are $\alpha=0.2$, $\beta=0.2$, and $\gamma=9$ [19]. The Jacobian matrix is

$$\mathbf{DF}=\begin{pmatrix}0 & -1 & -1\\ 1 & \alpha & 0\\ z & 0 & x-\gamma\end{pmatrix}.\tag{8}$$

The Lyapunov exponents for the this system are $\lambda_1\simeq0.080$, $\lambda_2\simeq0$, and $\lambda_3\simeq-8.716$. The MSFs under various coupling schemes are shown in Fig. 1.

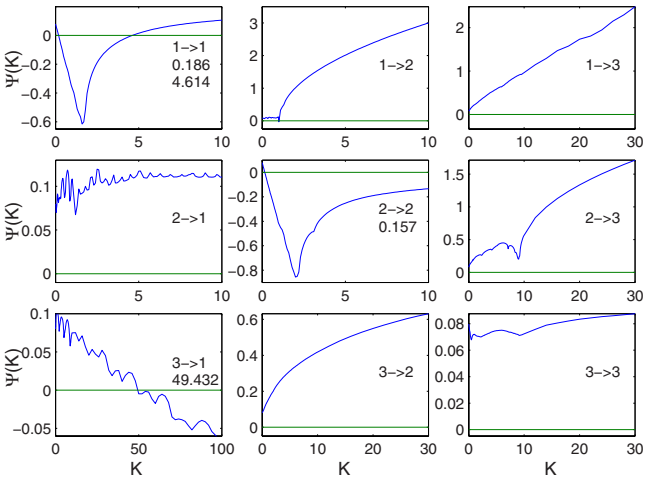

FIG. 1. (Color online) For the chaotic Rössler oscillator [Eq. (7)], MSFs versus the normalized coupling parameter K under various coupling schemes. In each panel, the notation $i\to j$ indicates the coupling as being from the ith component of one oscillator to the jth component of another oscillator. The numerical values below the $i\to j$ notion indicate the K values at which $\Psi(K)$ changes sign. The same notation is applied for subsequent Fig. 2 through Fig. 8. Parameter setting is specified in the text.

2. Lorenz system

Here,

$$\begin{cases}\dot{x}=\sigma(y-x)\\ \dot{y}=x(\rho-z)-y\\ \dot{z}=xy-\beta z,\end{cases}\tag{9}$$

where $\sigma=10$, $\rho=28$, and $\beta=2$ [20]. The Jacobian matrix is

$$\mathbf{DF}=\begin{pmatrix}-\sigma & \sigma & 0\\ \rho-z & -1 & -x\\ y & x & -\beta\end{pmatrix}.\tag{10}$$

The Lyapunov exponents are $\lambda_1\simeq0.819$, $\lambda_2\simeq0$, and $\lambda_3\simeq-13.819$. Since the diagonals of the Jacobian matrix are independent of the dynamical variables, the sum of the Lyapunov exponents is equal to the trace of the Jacobian matrix **DF**. Indeed, we have $\lambda_1+\lambda_2+\lambda_3\simeq-13$ and $\mathrm{Tr}(\mathbf{DF})=-\sigma-1-\beta=-13$. The MSFs for different coupling schemes are shown in Fig. 2 for $\beta=2$ and in Fig. 3 for $\beta=8/3$. Note that the MSF for $3\to3$ coupling is a generalization of the Turing bifurcation [30].

3. Chen's system

Here,

$$\begin{cases}\dot{x}=a(y-x)\\ \dot{y}=(c-a-z)x+cy\\ \dot{z}=xy-\beta z,\end{cases}\tag{11}$$

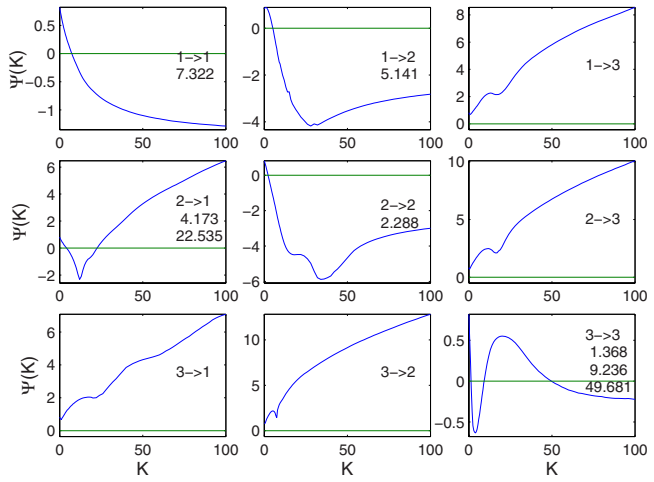

FIG. 2. (Color online) For the chaotic Lorenz system [Eq. (9)] for $\beta=2$, MSFs versus the normalized coupling parameter K under different coupling schemes.

where $a=35$, $c=28$, and $\beta=8/3$ [21]. The Jacobian matrix is

$$\mathbf{DF} = \begin{pmatrix} -a & a & 0 \\ c-a-z & c & -x \\ y & x & -\beta \end{pmatrix}. \tag{12}$$

The Lyapunov exponents are $\lambda_1 \simeq 2.154$, $\lambda_2 \simeq 0$, and $\lambda_3 \simeq -11.820$. The sum of the Lyapunov exponents is equal to $\mathrm{Tr}(\mathbf{DF}) = -a+c-\beta \simeq -9.667$. Note that for our calculation, Eq. (5) is integrated together with Eq. (1) using the RK4 method. If Eq. (5) is integrated using the Euler method while Eq. (1) is integrated using RK4 method, the calculated Lyapunov exponents are $\lambda_1 \simeq 2.17$, $\lambda_2 \simeq 0.25$, and $\lambda_3 \simeq -11.96$. This can lead to systematic errors. The MSFs of this system as a function of the generalized parameter K are shown in Fig. 4.

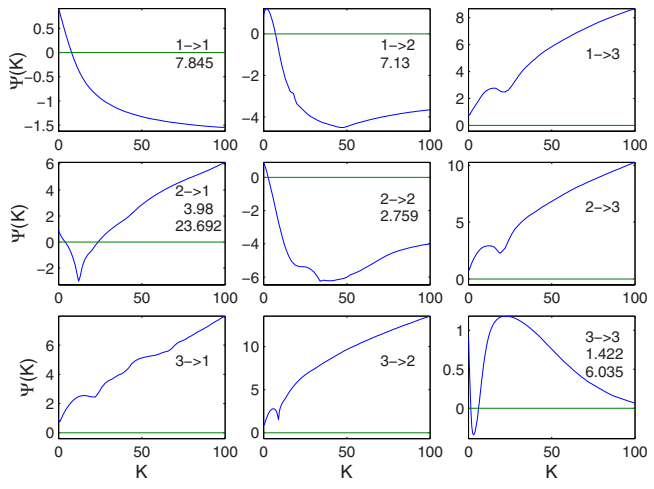

FIG. 3. (Color online) For the chaotic Lorenz system [Eq. (9)] for $\beta=8/3$, MSFs versus the normalized coupling parameter K under different coupling schemes.

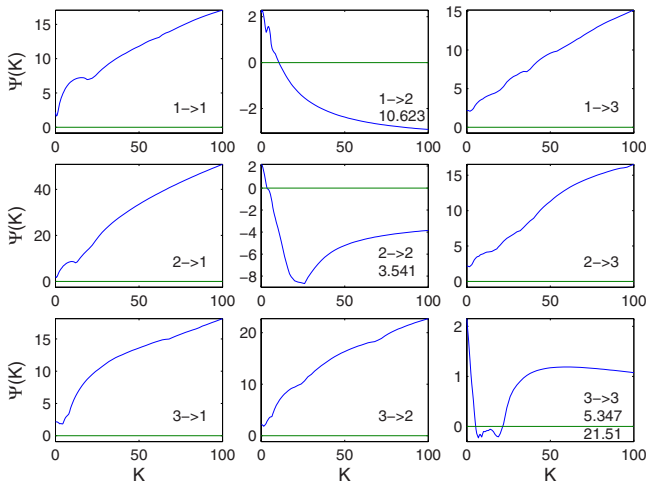

FIG. 4. (Color online) For Chen's system [Eq. (11)], MSFs versus the normalized coupling parameter K under different coupling schemes.

4. Chua's circuit system

Here,

$$\begin{cases} \dot{x} = \alpha[y - x + f(x)] \\ \dot{y} = x - y + z \\ \dot{z} = -\beta y - \gamma z, \end{cases} \tag{13}$$

where $\alpha=10$, $\beta=14.87$, $\gamma=0$, and

$$f(x) = \begin{cases} -bx - a + b, & x > 1 \\ -ax, & |x| < 1 \\ -bx + a - b, & x < -1, \end{cases} \tag{14}$$

where $a=-1.27$ and $b=-0.68$ [22]. The Jacobian matrix is

$$\mathbf{DF} = \begin{pmatrix} -\alpha - \alpha \times \begin{cases} b, |x| > 1 \\ a, |x| < 1 \end{cases} & \alpha & 0 \\ 1 & -1 & 1 \\ 0 & -\beta & -\gamma \end{pmatrix}. \tag{15}$$

The Lyapunov exponents for this system are $\lambda_1 \simeq 0.409$, $\lambda_2 \simeq 0$, and $\lambda_3 \simeq -3.859$. The behaviors of the MSFs under different coupling schemes are presented in Fig. 5.

5. HR neuron

Here,

$$\begin{cases} \dot{x} = y + 3x^2 - x^3 - z + I \\ \dot{y} = 1 - 5x^2 - y \\ \dot{z} = -rz + rs(x + 1.6), \end{cases} \tag{16}$$

where $I=3.2$ is the external current input, $r=0.006$, and $s=4$ [23]. The Jacobian matrix is

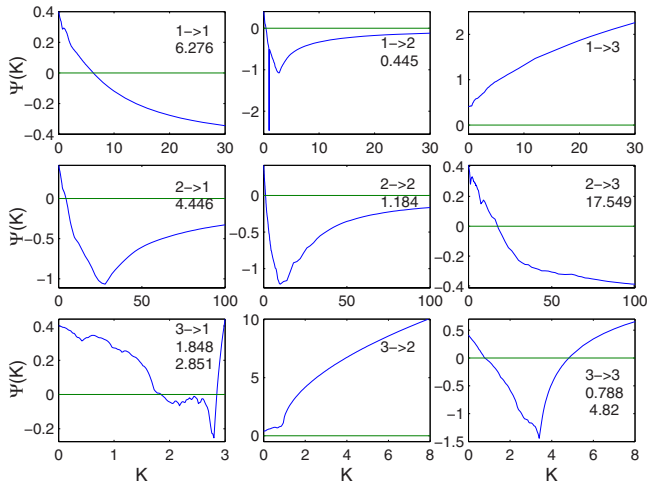

FIG. 5. (Color online) For the Chua circuit system [Eq. (13)], MSFs versus the normalized coupling parameter K under different coupling schemes.

$$\mathbf{DF} = \begin{pmatrix} 6x - 3x^2 & 1 & -1 \\ -10x & -1 & 0 \\ rs & 0 & -r \end{pmatrix}. \tag{17}$$

The Lyapunov exponents are $\lambda_1 \simeq 0.013$, $\lambda_2 \simeq 0$, and $\lambda_3 \simeq -8.610$. The MSFs versus the normalized coupling parameter K under different coupling schemes are shown in Fig. 6.

6. Forced Duffing oscillator

Here,

$$\begin{cases} \dot{x} = y \\ \dot{y} = -hy - x^3 + q\,\sin(\eta t), \end{cases} \tag{18}$$

where $\eta = 1$, $h = 0.1$, and $q = 5.6$ [24]. The Jacobian matrix is

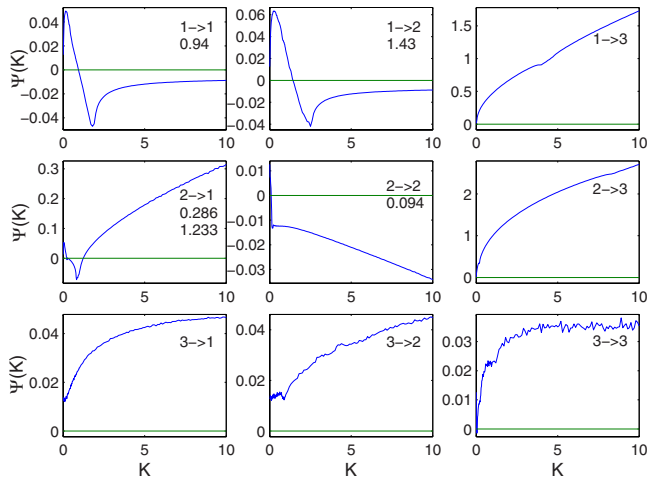

FIG. 6. (Color online) For the HR neuron system [Eq. (16)], MSFs versus the normalized coupling parameter K under different coupling schemes.

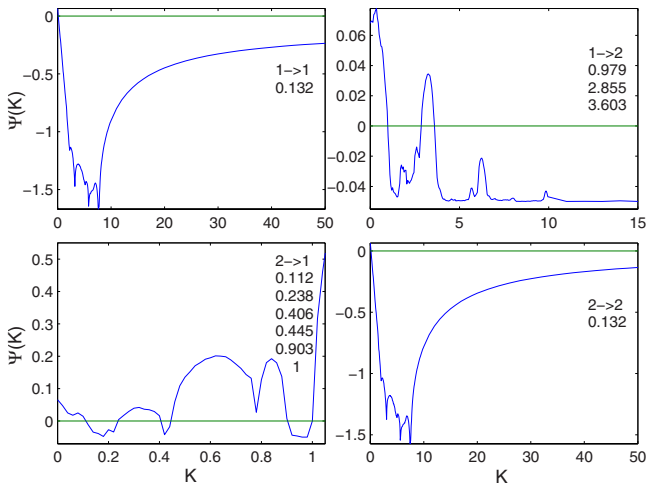

FIG. 7. (Color online) For the forced Duffing system [Eq. (18)] under different coupling schemes, MSFs versus the normalized coupling parameter K.

$$\mathbf{DF} = \begin{pmatrix} 0 & 1 \\ -3x^2 & -h \end{pmatrix}. \tag{19}$$

Considering the driven term as an extra dimension, i.e., $\dot{t} = 1$, the Lyapunov exponents are $\lambda_1 \simeq 0.066$, $\lambda_2 = 0$, and $\lambda_3 \simeq -0.166$. The sum of the exponents is equal to $\mathrm{Tr}(\mathbf{DF}) = -h = 0.1$. The behaviors of various MSFs are shown in Fig. 7.

7. Forced van der Pol system

Here,

$$\begin{cases} \dot{x} = y \\ \dot{y} = -x + d(1 - x^2)y + F\,\sin(\eta t), \end{cases} \tag{20}$$

where we use $d = 3$, $F = 15$, and $\eta = 4.065$ [25]. The Jacobian matrix is

$$\mathbf{DF} = \begin{pmatrix} 0 & 1 \\ -1 - 2dxy & d(1 - x^2) \end{pmatrix}. \tag{21}$$

Considering an extra equation $\dot{t} = 1$, the Lyapunov exponents for the this system are $\lambda_1 \simeq 0.106$, $\lambda_2 = 0$, and $\lambda_3 \simeq -2.774$. The MSFs versus the normalized coupling parameter under various coupling schemes are presented in Fig. 8.

C. Classification of MSFs

Based on the numerical results in Sec. III B, we propose a general scheme to classify the behaviors of the MSFs in typical low-dimensional nonlinear oscillators in terms of the behaviors of $\Psi(K)$ crossing the K axis [31]. In particular, let Γ_n be the class where $\Psi(K)$ has n cross points with the K axis. For a chaotic oscillator, the value of the MSF for $K = 0$ is the largest Lyapunov exponent of the oscillator, which is positive and assumes the same value under different coupling schemes. Several important classes are in order:

(1) Class Γ_0: $\Psi(K)$ has no finite cross points with K axis, hence $\Psi(K)$ is always positive, and a coupled network of such oscillators does not allow any synchronization state.

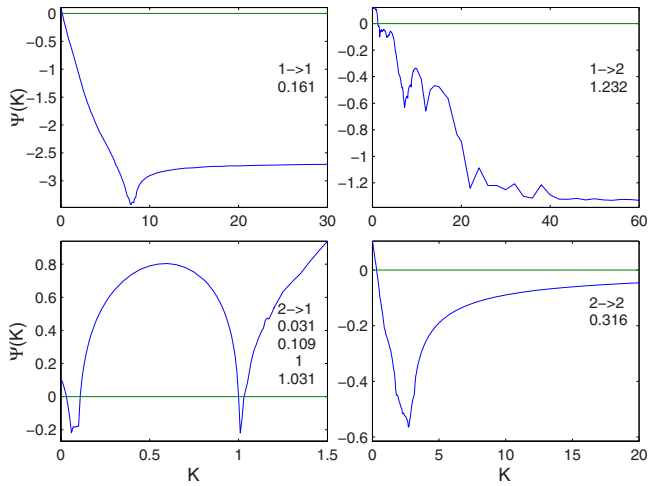

FIG. 8. (Color online) For the forced van der Pol system [Eq. (20)] under various coupling schemes, MSFs versus the normalized coupling parameter K.

(2) Class Γ_1: $\Psi(K)$ has only one finite cross point K_a. After crossing the K axis at K_a, $\Psi(K)$ remains negative for all $K>K_a$. For this class, the coupled network of oscillators will synchronization once $K_2=\varepsilon\mu_2>K_a$, where μ_2 is the smallest nontrivial eigenvalue of the coupling matrix $\mathbf{G}$.

(3) Class Γ_2: $\Psi(K)$ possesses two finite cross points, K_a and K_b, with the K axis, where $K_a<K_b$. For this class, $\Psi(K)$ becomes negative at K_a and as K is increased and $\Psi(K)$ becomes positive again at K_b and remain positive thereafter. In this case, $\Psi(K)$ is negative in a finite interval (K_a,K_b). The synchronization condition for such coupled oscillator system is $K_a<\varepsilon\mu_2$ and $K_b>\varepsilon\mu_N$, where μ_N is the largest eigenvalue of the coupling matrix $\mathbf{G}$.

(4) Class Γ_3: $\Psi(K)$ has three finite cross points K_{a1},K_{b1}, K_{a2}. For this class, the coupled oscillator system is synchronizable if the eigenvalues of the coupling matrix satisfy that $\varepsilon\mu_i, i=2,\ldots,N$ all reside in the intervals (K_{a1},K_{b1}) and (K_{a2},∞), i.e., for general cases there exists certain j, where $j=3,\ldots,N-1$, satisfying the following relations: $K_{a1}<\varepsilon\mu_2$ and $K_{b1}>\varepsilon\mu_j$, and $K_{a2}<\varepsilon\mu_{j+1}$; or in the extreme case, all $\varepsilon\mu_i$s reside in one interval, i.e., $K_{a1}<\varepsilon\mu_2$ and $K_{b1}<\varepsilon\mu_N$, or $\varepsilon\mu_2>K_{a2}$. This is of particular interest for ragged synchronization problems [24]. Similar arguments hold for class Γ_n, $n=5,7,\ldots$. A common feature for these odd classes is that when the coupling is strong enough $(\varepsilon>K_n/\mu_N)$, the system can always be synchronized.

(5) Class Γ_n, where $n=4,6,\ldots$: $\Psi(K)$ has n finite cross points, which can be grouped into (K_{a1},K_{b1}), $(K_{a2},K_{b2}),\ldots,$ $(K_{am},K_{bm}=K_n)$, where $m=n/2$. For these classes, synchronization of the coupled oscillators can be more intricate, i.e., only when $\varepsilon\mu_i, i=2,\ldots,N$ all reside in the $n/2$ intervals. They can be all in one interval, or they can spread in all these $n/2$ intervals. For these even classes, strong coupling, e.g., $\varepsilon>K_n/\mu_N$, will lead to desynchronization.

Varying system parameters may change the class of a particular MSF. However, since the limit behavior of MSF for large K is locally robust (it cannot be globally robust as the attractor can be totally destroyed if a parameter changes significantly), the cross points with K axis are usually generated or annihilated in pairs, thus the MSF can jump from one class to another with the same parity, i.e., from even to even or from odd to odd. For example, for the forced Duffing oscillator [Eq. (18)] with $1\rightarrow2$ coupling, increasing q to 11.3 will change the MSF from Γ_3 to Γ_5. That is, the parity of the MSFs is preserved when the parameter of the system changes. Note that some MSFs are generalizations of the Turing bifurcation, i.e., the MSF of Lorenz oscillator for $3\rightarrow3$ coupling, and all Turing bifurcations preserve the parity of class. It is unclear that whether the limit of MSF can change sign abruptly through bifurcation or change gradually via an asymptote to zero, but this is usually accompanied with structural metamorphosis of the attractor itself. Therefore, we conjecture that the classification is structurally stable and that such zero asymptotes are isolated points in parameter space.

For the seven types of oscillators that we have studied, the classification is summarized in Table I. A general finding is that, for most oscillators, there exists a coupling configuration for which the MSF is negative in a finite parameter interval (belong to even classes).

IV. ASYMPTOTIC BEHAVIOR OF MSF

The behavior of the MSF $\Psi(K)$ in the large-K limit for diagonal couplings has been discussed by Fink *et al.* [32], which is determined by the sub-block Lyapunov exponents. Here we shall focus on the nondiagonal couplings and determine the asymptotic behavior of $\Psi(K)$ for large K values. Without loss of generality, we assume the dimensionality of the oscillator to be $d=3$. The Jacobian matrix of the oscillators with respect to the synchronization manifold is denoted by

TABLE I. Classification based on master stability functions.

Class	Rössler	Lorenz	Chen	Chua	HR	Duffing	Van der Pol
Γ_0	$1\rightarrow2,1\rightarrow3,2\rightarrow1,$ $2\rightarrow3,3\rightarrow2,3\rightarrow3$	$1\rightarrow3,2\rightarrow3,3\rightarrow1,$ $3\rightarrow2$	$1\rightarrow1,1\rightarrow3,2\rightarrow1,$ $2\rightarrow3,3\rightarrow1,3\rightarrow2$	$1\rightarrow3,3\rightarrow2$	$1\rightarrow3,2\rightarrow3,3\rightarrow1,$ $3\rightarrow2,3\rightarrow3$		
Γ_1	$2\rightarrow2,3\rightarrow1$	$1\rightarrow1,1\rightarrow2,2\rightarrow2$	$1\rightarrow2,2\rightarrow2$	$1\rightarrow1,1\rightarrow2,2\rightarrow1,$ $2\rightarrow2,2\rightarrow3$	$1\rightarrow1,1\rightarrow2,$ $2\rightarrow2$	$1\rightarrow1,$ $2\rightarrow2$	$1\rightarrow1,1\rightarrow2,$ $2\rightarrow2$
Γ_2	$1\rightarrow1$	$2\rightarrow1$	$3\rightarrow3$ [33]	$3\rightarrow1,3\rightarrow3$	$2\rightarrow1$		
$\Gamma_{3,5,\ldots}$		$3\rightarrow3$				$1\rightarrow2$	
$\Gamma_{4,6,\ldots}$						$2\rightarrow1$	$2\rightarrow1$

$$\mathbf{DF} = \begin{pmatrix} a_{11} & a_{12} & a_{13} \\ a_{21} & a_{22} & a_{23} \\ a_{31} & a_{32} & a_{33} \end{pmatrix}, \tag{22}$$

where a_{ij} depends on the system variables. The matrix that determines the MSF is

$$\mathbf{DF} - K\mathbf{DH}, \tag{23}$$

where K is the normalized coupling parameter. For one-component coupling, there is only one nonzero element in **DH**. To gain insights, we assume that for large K, **DF** can be approximated by a constant matrix, where each element a_{ij} is assumed to be its time-averaged value associated with the asymptotic trajectory. Thus the variational Eq. (4) can be approximated by a linear system, and the MSF is the largest real eigenvalue of the matrix $\mathbf{DF}-K\mathbf{DH}$, which is determined by

$$\mathrm{Det}(\lambda\mathbf{I} - \mathbf{DF} + K\mathbf{DH}) = 0, \tag{24}$$

where I is a 3×3 unit matrix. From numerical simulations, we have observed that, for nondiagonal coupling, the MSFs in many cases have the form of powers of K in the large K limit. Assume the coupling is from the jth component of one oscillator to the ith component of another oscillator, we have $(\mathbf{DH})_{kl} = \delta_{ik}\delta_{jl}$. For $K \gg 0$, we assume that the solution of Eq. (24) with largest real part, $\lambda_{\max}$, has the form

$$\lambda_{\max} \sim K^{\alpha}. \tag{25}$$

Thus expanding Eq. (24) and for large K, the terms without K or $\lambda_{\max}$ could be neglected. We obtain the following approximate equation for $\lambda_{\max}$:

$$\lambda_{\max}^3 - \sum_{n=1}^{3} a_{nn}\lambda_{\max}^2 + a_{ji}K\lambda_{\max} - (a_{ji}a_{hh} - a_{jh}a_{hi})K \approx 0, \tag{26}$$

where h is the index that is not equal to i or j (note that $i \neq j$ since the coupling is nondiagonal). We then have for $a_{ji} < 0$,

$$\Psi(K) = \lambda_{\max} \approx \sqrt{-a_{ji}}\sqrt{K}, \tag{27}$$

for $a_{ji}=0$ and $a_{jh}a_{hi} < 0$,

$$\Psi(K) = \lambda_{\max} \approx \sqrt[3]{-a_{jh}a_{hi}}\sqrt[3]{K}, \tag{28}$$

and for $a_{ji}=0$ and $a_{jh}a_{hi} > 0$, the root that is similar to Eq. (28) is now negative, thus it is the conjugate root with imaginary part that has the largest positive part. We have

$$\Psi(K) = \mathrm{Re}\{\lambda_{\max}\} \approx \frac{1}{2}\sqrt[3]{a_{jh}a_{hi}}\sqrt[3]{K}. \tag{29}$$

However, for $a_{ji} > 0$, $\Psi(K)$ is not in the form of powers of K for large K. Note that for coupling from the jth component of one oscillator to the ith component of another oscillator, only the $a_{ji}K\lambda_{\max}$ and $(-a_{jh}a_{hi})K$ terms contain K. For $a_{ji} \neq 0$, since the power of K in the term $(-a_{jh}a_{hi})K$ is less than that in the term $a_{ji}K\lambda_{\max}$, the former can be neglected. The asymptotic behavior is affected by the term a_{ji}, as shown in Eq. (27). If $a_{ji}=0$ and $a_{jh}a_{hi} \neq 0$, $\lambda_{\max}$ will be determined by the term $-a_{jh}a_{hi}K$, leading to the asymptotic behaviors as given by Eqs. (28) and (29). Moreover, if $a_{ji}=0$ and $a_{jh}a_{hi}=0$, $\lambda_{\max}$ does not depend on K, leading to a constant value for $\Psi(K)$. However, none of the systems that we have tested falls into this special category.

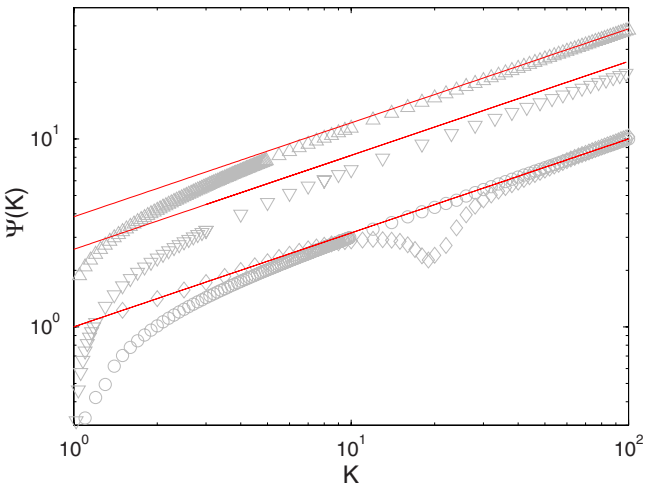

FIG. 9. (Color online) Behaviors of MSFs for $a_{ji} < 0$. Circles: Rössler system under $1 \to 2$ coupling; diamonds: Lorenz system under $2 \to 3$ coupling; up-triangles: Chua circuit under $3 \to 2$ coupling; down-triangles: forced Duffing system under $2 \to 1$ coupling. Solid straight lines are from Eq. (27).

We now present several examples to validate the asymptotic behavior of the MSF in the large coupling limit as suggested by our heuristic analysis. First, we show the case of $a_{ji} < 0 (i \neq j)$ in Fig. 9 where circles, diamonds, up-triangle, and down-triangle are the MSFs of different chaotic oscillators under different coupling schemes. It can be seen that the behaviors of MSFs agree with those predicted by our analysis. Next, we investigate the case of $a_{ji}=0$, which is relatively rare in the systems that we have investigated. In particular, the Rössler system under $3 \to 2$ coupling, the Chua circuit under $3 \to 1$ coupling, and the HR neuron system under $2 \to 3$ and $3 \to 2$ couplings belong to this category. The corresponding MSFs are shown in Fig. 10. We again observe a reasonable agreement between theory and numerics.

From our computations, we also find that there are cases where $\Psi(K)$ approaches asymptotically a constant value. For example, for the forced Duffing system under $1 \to 2$ coupling, $\Psi(K)$ approaches -0.05. The reason for this behavior is that in these cases, for large K, the governing matrix $\mathbf{DF} - K\mathbf{DH}$ is approximately a constant matrix. Thus from Eqs. (5) and (6), the Lyapunov exponents are given by the real parts of the eigenvalues of the governing matrix. Since Ks being large only affects the imaginary part of the eigenvalues, the largest Lyapunov exponent is a constant. For example, in the forced Duffing system under $1 \to 2$ coupling, the governing matrix is

$$\mathbf{DF} - K\mathbf{DH} = \begin{pmatrix} 0 & 1 \\ -3x^2 - K & -h \end{pmatrix} \approx \begin{pmatrix} 0 & 1 \\ -K & -h \end{pmatrix} \tag{30}$$

for large K. Then, the eigenvalues are

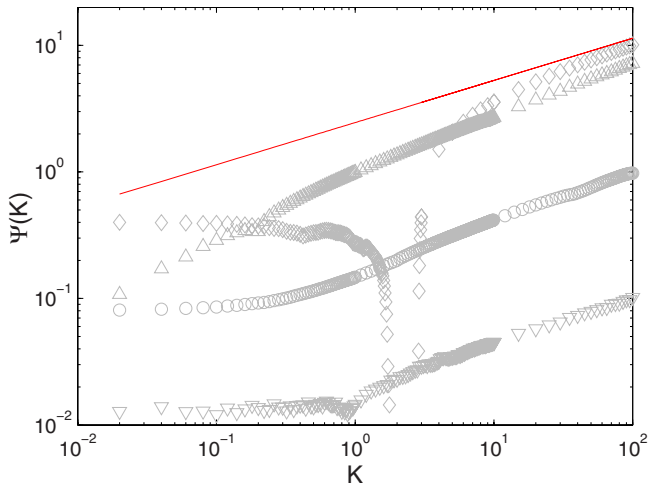

FIG. 10. (Color online) Behaviors of MSFs for $a_{ji}=0$. Circles: Rössler system under $3\rightarrow 2$ coupling; diamonds: Chua circuit under $3\rightarrow 1$ coupling; up-triangle: HR neuron under $2\rightarrow 3$ coupling; down-triangle: HR neuron under $3\rightarrow 2$ coupling. The solid line is from Eq. (28) for Chua circuit under $3\rightarrow 1$ coupling.

$$\frac{-h+i\sqrt{4K-h^2}}{2}, \tag{31}$$

and the largest real part is $h/2$. As a result, we have $\Psi(K)\approx -h/2=-0.05$ for large K.

Using the eigenvalue analysis, certain critical K values leading to $\Psi(K)=0$ can be obtained in the forced Duffing and the forced van der Pol oscillators. For example, for the forced Duffing oscillator under $2\rightarrow 1$ coupling, the governing matrix is

$$\begin{pmatrix} 0 & 1-K \\ -3x^2 & -h \end{pmatrix}. \tag{32}$$

For $K=1$, the governing matrix degenerates and the largest eigenvalue becomes zero, indicating that there exists a synchronizable region in K about this value. Numerical evidence of the existence of such a point is shown in Fig. 7. In the forced van der Pol oscillator under the $2\rightarrow 1$ coupling scheme, a similar behavior has been observed.

V. SIMULATION OF ACTUAL SYNCHRONIZATION DYNAMICS

The MSF formalism provides a general criterion for determining the synchronizability of a system of coupled nonlinear oscillators. It is insightful to perform direct numerical simulations of synchronization dynamics and compare results with those indicated by the MSFs. Since the role of the coupling matrix in affecting the stability of the synchronization state is reflected only by the eigenvalues, it suffices to consider a system of two coupled oscillators, for which the coupling matrix is simply

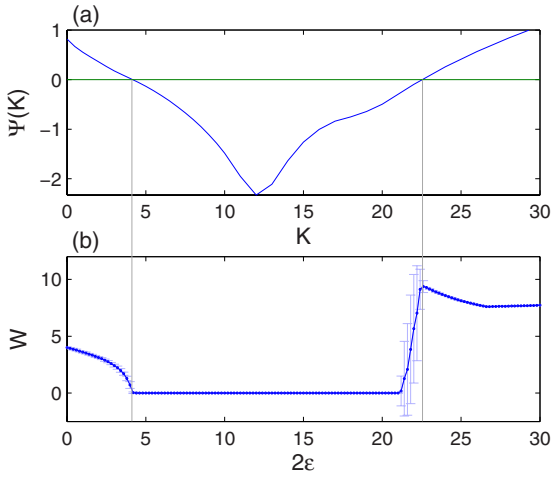

FIG. 11. (Color online) For a system of two coupled Lorenz oscillators under $2\rightarrow 1$ coupling, (a) MSF and (b) synchronization indicator W as a function of the normalized coupling parameter $K=2\varepsilon$.

$$\mathbf{G}=\begin{pmatrix} 1 & -1 \\ -1 & 1 \end{pmatrix}. \tag{33}$$

The eigenvalues are 0 and 2. We thus have $K=2\varepsilon$, and the synchronization condition is given by $\Psi(2\varepsilon)<0$. Generally, one can use the difference in the state variables between the oscillators to characterize synchronization. For example, we can examine the fluctuation width defined by $W=\langle\langle|x_i-\langle x_j\rangle|\rangle_T\rangle_e$, where both time and ensemble averages are used. If the oscillator system is synchronized, then $x_1=x_2$ and $W=0$. Otherwise, W can assume large values.

Figure 11(b) shows W versus the coupling parameter ε for the Lorenz system under $2\rightarrow 1$ coupling. Figure 12(b) is the same plot for the Lorenz system under $3\rightarrow 3$ coupling. Results of the HR neuron system under $2\rightarrow 1$ coupling is shown in Fig. 13(b). The respective behaviors of the corre-

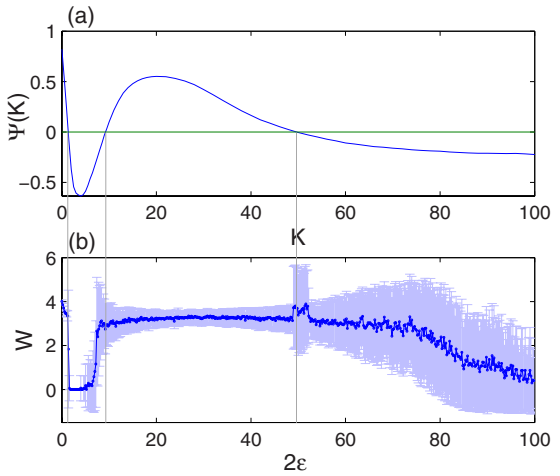

FIG. 12. (Color online) For a system of two coupled Lorenz oscillators under $3\rightarrow 3$ coupling, (a) MSF and (b) synchronization indicator W as a function of the normalized coupling parameter $K=2\varepsilon$.

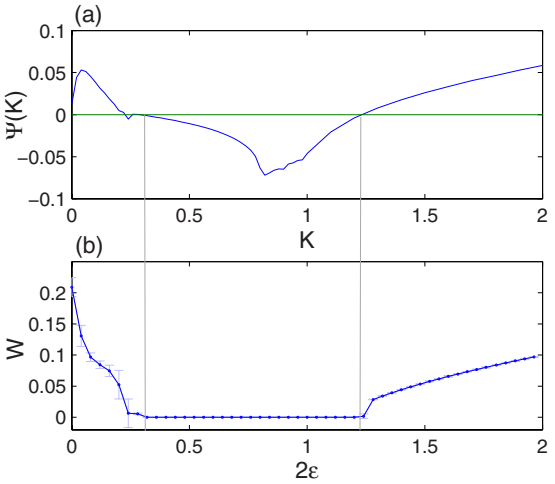

FIG. 13. (Color online) For a system of two coupled HR neurons under $2\rightarrow1$ coupling, (a) MSF and (b) synchronization indicator W as a function of the normalized coupling parameter $K=2\varepsilon$.

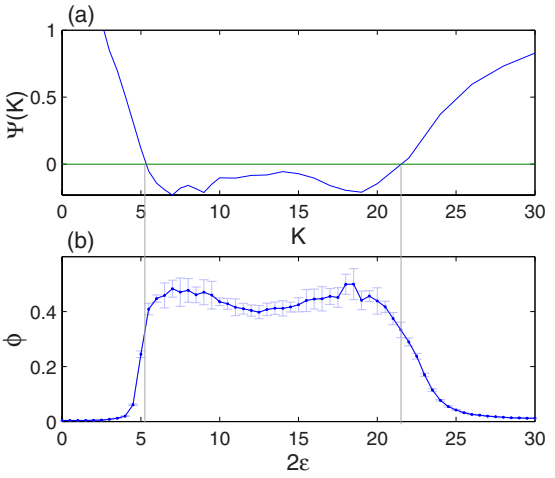

FIG. 14. (Color online) For the system of two coupled Chen's oscillators under $3\rightarrow3$ coupling scheme, (a) MSF and (b) actual simulation result of the fraction of synchronized time ϕ versus the normalized coupling parameter $K=2\varepsilon$.

sponding MSFs are also shown in these figures for comparison. In our simulations, we first run 10^4 time units to rid the system of any transient behavior and then use the following 10^3 time units to calculate W. An ensemble of 100 random initial conditions is used, which yields the average value W and the standard deviation. For values of ε for which the MSF is negative $[\Psi(2\varepsilon)<0]$, W is generally of the order of 10^{-8}, indicating complete synchronization in the coupled system. Since the MSF analysis is meaningful for initial conditions chosen in the neighborhood of the synchronization state in the phase space, as 2ε approaches the value for $\Psi(2\varepsilon)=0$ from the negative side, the volume of this attractive region approaches zero. Thus, about this critical value of ε, even if $\Psi(2\varepsilon)<0$, a finite initial disturbance can push the system out of the small attractive region, leading to destruction of synchronization. Such an example can be seen from Fig. 11(b) for values of ε close to $2\varepsilon=22.5$. Retrospectively, this sensitive dependence to the disturbance could be caused by riddled basins of the synchronization manifold near the desynchronization point, as has been demonstrated for x-coupled Rössler oscillators [34]. In general, however, we observe that the transition point indicated by W agrees well with that determined by the MSF.

For a system of coupled Chen's oscillators, an intermittent behavior between synchronization and desynchronization is observed. In this case, the quantity W is not proper to characterize the extent of synchronization. We use an alternative quantity, the fraction of synchronized time ϕ, to quantify synchronization, which is defined as the fraction of time that the difference in the state variables between oscillators, $\langle|x_i-\langle x_j\rangle|\rangle$, is smaller than a small threshold value, say 10^{-3}, during a long time interval. In the simulation, we first calculate 10^4 time units to allow the system to settle into the chaotic attractor and then calculate ϕ using 10^5 time units. An ensemble average of 100 realizations is also used. The results are shown in Fig. 14. Again, we observe a good agreement between the direct simulation result and that predicted by the MSF.

For the Chua's circuit model, divergence of trajectories is common. Thus neither W nor ϕ is useful for quantifying the degree of synchronization. To devise a suitable characterizing quantity, we note that, when a trajectory does not diverge and $\Psi(2\varepsilon)<0$, the coupled system can be synchronized and W is on the order of 10^{-8}. Thus we define P_{syn} as the probability that the coupled system does not diverge and synchronize. Numerically, this can be determined when the condition $\langle|x_i-\langle x_j\rangle|_T\rangle<10^{-3}$ is satisfied for a certain time period after entering the steady state. In our simulation, after disregarding a transient phase of 10^4 time units, we examine 10^3 time units to see if $\langle|x_i-\langle x_j\rangle|\rangle_T$ is smaller than 10^{-3} in this time interval. If yes, we deem this case as synchronizable. For each value of the coupling parameter ε, we use an ensemble of 1000 realizations to calculate P_{syn}, estimated as the fraction of the synchronized cases. Results are shown in Fig. 15. We observe that the direct-simulation results are consistent with the MSF predictions.

From both MSF calculations and numerical simulations of actual oscillator systems, we find that nondiagonal couplings

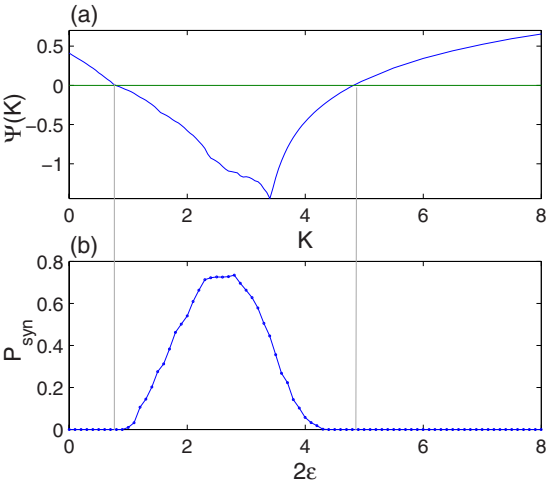

FIG. 15. (Color online) For the system of two coupled Chua's circuits under the $3\rightarrow3$ coupling scheme, (a) MSF and (b) direct simulation results of the synchronization probability P_{syn}.

can also lead to complete synchronization (see also [24,35]. This is surprising since the driven signal can be quite different from the target signal. For example, for coupled Rössler oscillators under $3 \rightarrow 1$ coupling [coupling from z component to x component, see Eq. (7)], synchronization can arise if the coupling parameter is large. The time series of the z component is pulselike, while the evolution of the x component resembles that of a regular sinusoidal wave. The nondiagonal coupling induced synchronization prevails in most of the coupled oscillator systems studied in Sec. III B (Table I).

MSFs are structurally stable, i.e., their properties are invariant under small parameter variations. They, however, cannot be globally stable as oscillators with distinct parameters can have totally different attractor structures. Since MSFs represent local stability criterions, even if $\Psi \lesssim 0$, the coupled system can exhibit behaviors other than synchronization, depending on the properties of the chaotic attractor. In our direct simulations, we observe that, while there are cases where the difference of the dynamical variables decreases to zero as soon as Ψ becomes negative, there are also other cases where a gradual transition in the characterizing quantity of synchronization occurs. In any case, our direct-simulation results suggest that the system generally synchronizes better if the MSF is more negative, and the transition to synchronization can usually be predicted well by the behavior of the MSF. While here we have used the largest Lyapunov exponent as the measure of MSF, we suspect that using other stronger measures, such as the stability of one or more of the lower unstable periodic orbits could yield better indicators of actual synchronization. These issues will be explored in future works.

VI. CONCLUSION

We have systematically examined known low-dimensional chaotic oscillators and analyzed the corresponding MSFs under all one-component coupling schemes. We find that, for most of these oscillators, there exist some coupling schemes that lead to MSFs being negative in a finite interval of the normalized coupling parameter, a property that has been assumed tacitly in the literature of network synchronization. In fact, MSFs can exhibit a variety of different behaviors, which can be conveniently categorized into four classes. Results from direct calculations of appropriate synchronization measures for different systems indicate that the MSF framework is effective for probing the transition to synchronization in systems of coupled nonlinear oscillators.

ACKNOWLEDGMENT

This work was supported by ONR under Grant No. N00014-08-1-0627.

[1] L. M. Pecora and T. L. Carroll, Phys. Rev. Lett. **64**, 821 (1990).
[2] K. M. Cuomo and A. V. Oppenheim, Phys. Rev. Lett. **71**, 65 (1993).
[3] J. F. Heagy, T. L. Carroll, and L. M. Pecora, Phys. Rev. E **50**, 1874 (1994).
[4] N. F. Rulkov, M. M. Sushchik, L. S. Tsimring, and H. D. I. Abarbanel, Phys. Rev. E **51**, 980 (1995).
[5] M. G. Rosenblum, A. S. Pikovsky, and J. Kurths, Phys. Rev. Lett. **76**, 1804 (1996).
[6] L. M. Pecora and T. L. Carroll, Phys. Rev. Lett. **80**, 2109 (1998).
[7] S. Strogatz, *Sync: The Emerging Science of Spontaneous Order* (Hyperion, New York, 2003).
[8] A. S. Pikovsky, M. G. Rosenblum, and J. Kurths, *Synchronization: A Universal Concept in Nonlinear Sciences* (Cambridge University Press, New York, 2003).
[9] M. Barahona and L. M. Pecora, Phys. Rev. Lett. **89**, 054101 (2002).
[10] D. J. Watts and S. H. Strogatz, Nature (London) **393**, 440 (1998).
[11] T. Nishikawa, A. E. Motter, Y.-C. Lai, and F. C. Hoppensteadt, Phys. Rev. Lett. **91**, 014101 (2003).
[12] M. Chavez, D.-U. Hwang, A. Amann, H. G. E. Hentschel, and S. Boccaletti, Phys. Rev. Lett. **94**, 218701 (2005).
[13] L. Donetti, P. I. Hurtado, and M. A. Muñoz, Phys. Rev. Lett. **95**, 188701 (2005).
[14] C. Zhou, A. E. Motter, and J. Kurths, Phys. Rev. Lett. **96**, 034101 (2006).
[15] C. Zhou and J. Kurths, Phys. Rev. Lett. **96**, 164102 (2006).
[16] L. Huang, K. Park, Y.-C. Lai, L. Yang, and K. Yang, Phys. Rev. Lett. **97**, 164101 (2006).
[17] D.-H. Kim and A. E. Motter, Phys. Rev. Lett. **98**, 248701 (2007).
[18] An alternative approach to analyzing network synchronizability is the connection-graph stability method. See, V. Belykh, I. Belykh, and M. Hasler, Physica D **195**, 159 (2004); I. Belykh, M. Hasler, M. Lauret, and H. Nijmeijer, Int. J. Bifurcation Chaos Appl. Sci. Eng. **15**, 3423 (2005); V. Belykh, I. Belykh, and M. Hasler, Physica D **224**, 42 (2006).
[19] O. E. Rössler, Phys. Lett. A **57**, 397 (1976).
[20] E. N. Lorenz, J. Atmos. Sci. **20**, 130 (1963).
[21] G. Chen and T. Ueta, Int. J. Bifurcation Chaos Appl. Sci. Eng. **9**, 1465 (1999).
[22] T. Matsumoto, L. O. Chua, and M. Komuro, IEEE Trans. Circuits Syst. **32**, 797 (1985).
[23] M. Dhamala, V. K. Jirsa, and M. Ding, Phys. Rev. Lett. **92**, 028101 (2004).
[24] A. Stefański, P. Perlikowski, and T. Kapitaniak, Phys. Rev. E **75**, 016210 (2007).
[25] R. Mettin, U. Parlitz, and W. Lauterborn, Int. J. Bifurcation Chaos Appl. Sci. Eng. **3**, 1529 (1993).
[26] If the coupling is mutual and equal, the resulting coupling matrix is symmetric which can be diagonalized with a set of real eigenvalues. Certain weighted, asymmetric coupling matrix could also yield a set of real eigenvalues, see, for example, Ref. [14].
[27] J. Jost and M. P. Joy, Phys. Rev. E **65**, 016201 (2001).

[28] E. Ott, *Chaos in Dynamical Systems* (Cambridge University Press, New York, 1993).
[29] J.-P. Eckmann and D. Ruelle, Rev. Mod. Phys. **57**, 617 (1985).
[30] A. Turing, Philos. Trans. R. Soc. London, Ser. B **237**, 37 (1952).
[31] We have noticed that there exist different classifications of the coupled dynamical behaviors [24,36] focusing on different points. Our extensive calculations with various chaotic oscillators show, however, that our classification scheme is more appropriate in the current context.
[32] K. S. Fink, G. Johnson, T. Carroll, D. Mar, and L. Pecora, Phys. Rev. E **61**, 5080 (2000).
[33] Numeric calculation (up to $K=2000$) shows that the MSF for Chen's oscillator under $3\rightarrow 3$ coupling goes asymptotically to zero.
[34] J. F. Heagy, T. L. Carroll, and L. M. Pecora, Phys. Rev. Lett. **73**, 3528 (1994).
[35] M. Zhan, G. Hu, and J. Yang, Phys. Rev. E **62**, 2963 (2000).
[36] S. Boccaletti, V. Latora, Y. Moreno, M. Chavez, and D.-U. Hwang, Phys. Rep. **424**, 175 (2006).